Journal of Statistical Physics, Vol. 92, Nos. 3/4, 1998

Characterization of Stochastic Bifurcations in a Simple Biological Oscillator

Takashi Tateno[1]

Received November 24, 1997

This study of the effect of noise on bifurcations in a simple biological oscillator with a periodically modulated threshold uses the first-passage-time problem of the Ornstein–Uhlenbeck process with a periodic boundary to define the operator governing the transition of a threshold phase density. Stochastic phase-locking is analyzed numerically by evaluating the evolution of the probability density function of the threshold phase. A firing phase map in a noisy environment is extended to a stochastic kernel so that stochastic bifurcations can be investigated by spectral analysis of the kernel.

KEY WORDS: First-passage-time problem; integrate-and-fire model; Markov chain; Ornstein–Uhlenbeck process; phase-locking; spectral analysis.

1. INTRODUCTION

One of an organism's biological rhythms can be influenced by that organism's other rhythms and by external rhythms in the environment. Interaction between the rhythms can lead to an entrainment, or synchronization, and the rhythms will thus lock into a fixed phase relation. Any physical system in the real world is always affected by small stochastic fluctuations, such as those due to thermal noise, and the main objective of the work described in this paper was to study the effect of noise on the synchronization and phase-locking of biological rhythms.

One approach to the analysis of stochastic bifurcations is to observe qualitative changes of stationary probability densities. Transitions of

[1] NTT Basic Research Laboratories, 3-1 Morinosato Wakamiya, Atsugi-shi, Kanagawa 240-31, Japan; e-mail: tateno@will.brl.ntt.co.jp

0022-4715/98/0800-0675$15.00/0

topological structures—for instance, changes in the number of peaks in stationary densities—have been analyzed experimentally and numerically.[1] Those transitions are called phenomenological bifurcation.[2]

This paper takes a different approach to stochastic bifurcations. Grasman and Roerdink[3] studied the van der Pol type of relaxation oscillators with stochastic perturbations and explored the probability distribution function of the oscillation period by using a one-dimensional stochastic process. Tateno *et al.*[4] applied their method to a periodically forced van der Pol relaxation oscillator with an additive term. Doi *et al.*[5] used a spectral analysis of stochastic kernels to quantitatively characterize changes of the bifurcations in the invariant probability density functions. In this paper their approach is used for characterizing stochastic bifurcations, and the bifurcations of probability density are examined numerically.

Many rhythmic biological activities have been modeled by variously realistic oscillators, and one of the simplest is the integrate-and-fire model. Several versions of the model have been used to investigate rhythmic activities such as mitosis,[6] the activity of cardiac pacemaker cells,[7] and the firing of pacemaker neurons.[8] The neural integrate-and-fire model describes the membrane potential across a leaky, current-clamped membrane in terms of a state variable.

In each model an activity rises monotonically toward a threshold. When this threshold is reached, an "event" occurs—in a neural model, the event represents the firing of the neuron or the occurrence of a spike—after which the activity decays to a lower value. In present work this decay is assumed to be instantaneous and discontinuous.

The interaction between rhythms has previously been investigated by using integrate-and-fire models into which a time-varying (specifically, a periodic) modulation has been incorporated in one of two ways. In one kind of model the threshold is subjected to a time-varying modulation and there is no forced term.[9] In the other kind the activity is modulated by a forced term and the threshold is held constant.[10] The response characteristics of both kinds of models have been studied in detail, and this paper deals with the former kind in noisy environments. It also investigates the effect of an additive noise analytically and numerically.

In this paper the firing phase map used to analyze phase-locking patterns is first defined in a deterministic case and is then extended to a stochastic case in a noisy environment. That is, a stochastic kernel is defined. An operator derived from the stochastic kernel is then defined and used to analyze the evolution of the model responses in the parameter space. Stochastic bifurcations are characterized numerically by applying a spectral analysis to the kernel.

2. DETERMINISTIC RESPONSE CHARACTERISTICS

2.1. Integrate-and-Fire Model

Assume that the state point $x(t)$ increases to a threshold $\phi(t)$ and is governed by the following first-order differential equation:

$$\frac{dx(t)}{dt} = -\frac{x(t)}{\tau} + \beta \tag{1}$$

where both τ and β are parameters. Also assume that

$$x(0) = x_0 \tag{2}$$

where x_0 is an initial point. Once the state point reaches the threshold, it instantaneously and discontinuously resets to zero, and the process repeats:

$$x(t^+) = 0 \qquad \text{if} \quad x(t) = \phi(t) \tag{3}$$

Let the threshold be time-varying and periodically modulated in such a way that the state point can become synchronized to the threshold. In particular, let the threshold $\phi(t)$ be sinusoidally modulated with time:

$$\phi(t) = 1 + k \sin\{2\pi(t + \theta_0)\} \tag{4}$$

where $\theta_0 \in C$ ($\equiv[0\ 1)$) is the initial phase and the parameter k is the amplitude of the modulation. Note that in Eq. (4) the period and the mean amplitude of the threshold have been set to 1 because dimensionless parameters and variables are designated by normalization. Hence the parameter τ is the ratio of the frequency of the periodical modulation of the threshold to the frequency of the autonomous oscillator governed by Eq. (1). After the state point reaches the threshold, it instantaneously resets to zero and restarts its growth according to Eq. (1).

Before the state point reaches the threshold for the first time, the state variable $x(t)$ is a solution of Eqs. (1) and (2):

$$x(t) = \tau\beta(1 - \exp(-t/\tau)) + x_0 \exp(-t/\tau) \tag{5}$$

In the following we will assume that the initial value $x_0 = 0$. For the state point to reach the threshold the condition

$$\tau\beta > 1 - k \tag{6}$$

must be satisfied.

When the state point of Eq. (1) reaches the threshold N times for every M cycles of the periodical threshold modulation, we will call the response pattern a $M:N$ phase-locking. Figure 1 shows three examples of phase-locking patterns: 2:1, 1:1, and 1:2 phase-locking responses.

Although this paper will treat only $M:N$ ($M \leqslant N$) phase-locking cases, in specifying the parameter space it is often useful to make a calculation of deterministic phase-locking regions. Numerical and analytical methods like those used in refs. 9 and 10 are used in Appendix A to evaluate the $M:1$ phase-locking regions.

2.2. Deterministic Firing Time Maps

Responses of this model can be described by a sequence $\{t_n\}$ ($n = 1, 2,...$), where t_n is the time at which the state point has reached the threshold n times. Call such a sequence the firing time and suppose that t_n and t_{n+1} are successive firing times. Then the map $f: t_n \to t_{n+1}$ can be obtained by solving the equation

$$F(t_{n+1}) = G(t_n) \tag{7}$$

when

$$x(t_n^+) = 0 \tag{8}$$

where the functions $F(t)$ and $G(t)$ are defined by

$$F(t) = \exp(t/\tau)[\tau\beta - 1 - k \sin\{2\pi(t + \theta_0)\}] \tag{9}$$

$$G(t) = \tau\beta \exp(t/\tau) \tag{10}$$

If the function $F(t)$ is invertible and F^{-1} is defined in the range of $G(t)$, Eq. (7) can be rewritten

$$t_{n+1} = f(t_n) \tag{11}$$

where

$$f(t) = F^{-1}(G(t)) \tag{12}$$

In the parameter space (τ, β, k) there are three regions in which we can find response patterns that may or may not be phase-locked.[10]

Region I. $\tau\beta - 1 > k\sqrt{1 + (2\pi\tau)^2}$. In this case $F(t)$ is an invertible and monotonically increasing function, so $f(t)$ of Eq. (12) is well defined.

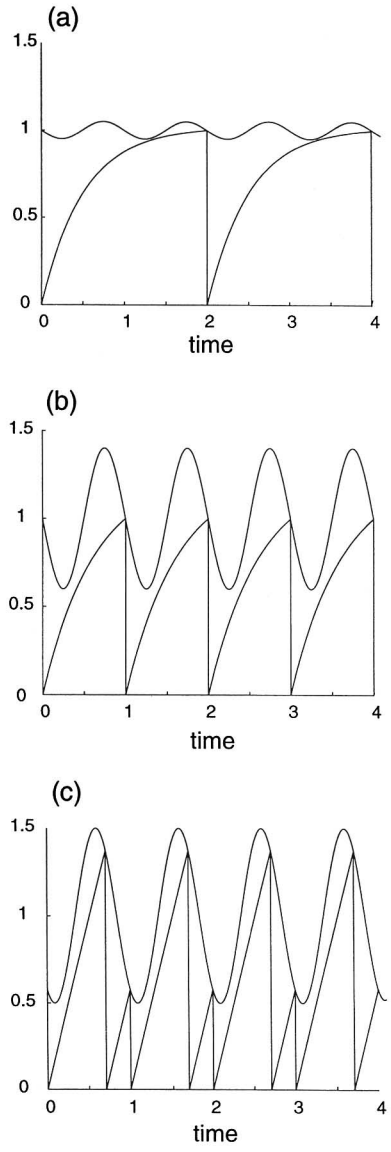

Fig. 1. Phase-locking patterns for the integrate-and-fire model with a sinusoidal threshold modulation. (a) 2:1 phase-locking, $\tau = 12.8$, $\beta = 2.0$, and $k = 0.05$; (b) 1:1 phase-locking, $\tau = 0.63$, $\beta = 2.0$, and $k = 0.4$; (c) 1:2 phase-locking, $\tau = 0.51$, $\beta = 2.0$, and $k = 0.5$. The parameter τ (defined in Section 2) represents the ratio of the frequency of the sinusoidal threshold modulation to the natural frequency of the unperturbed oscillator, and the parameter k is the amplitude of the threshold modulation.

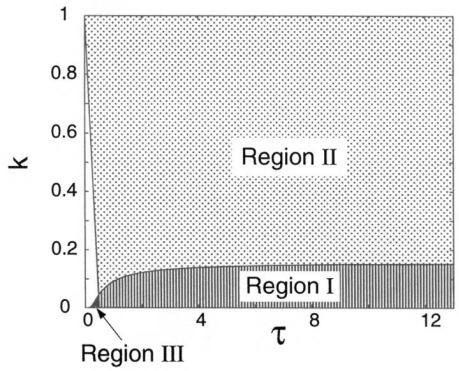

Fig. 2. The $k-\tau$ plane for a fixed parameter $\beta=2$. The parameter space can be divided into three regions according to the behavior of variable $x(t)$. In Region I we can find both quasi-periodic behavior and phase-locking patterns, but in Region II we cannot find quasi-periodic behavior. For the parameters in Region III the oscillating process will terminate.

In Region I the model behavior which does not correspond to phase-locking patterns is called quasi-periodic.

Region II. $k\sqrt{1+(2\pi\tau)^2} > |\tau\beta - 1|$. In this case the function $F(t)$ is not invertible, but the map $f: t_n \to t_{n+1}$ can still be defined from Eq. (7) if t_{n+1} is specified to be the smallest solution of Eq. (7) which is greater than t_n. In this region occurs a type of behavior quantitatively different from that occurring in Region I: the set of the parameter space in which the dynamical behavior does not correspond to phase-lockings is of measure zero.[10]

Region III. $1-\tau\beta > k\sqrt{1+(2\pi\tau)^2}$. In this region the function $F(t)$ is negative in the range of G and its relative maxima decrease as t increases. This means that the firing process defined by Eq. (1) terminates.

The parameter space can thus be divided into three distinct regions, which for the parameter $\beta=2$ are shown in Fig. 2.

2.3. Deterministic Firing Phase Maps

In this subsection a firing phase map is defined as a mapping from the phase of the threshold at one firing time to that at the next firing time. For a time interval $t \in R$ and $\psi_0 \in C$, a phase $\psi_1 \in C$ is defined as follows:

$$\psi_1 = t + \psi_0 \pmod 1 \tag{13}$$

$$\equiv \eta(t; \psi_0) \tag{14}$$

The notation $t+\psi(\mathrm{mod}\ 1)$ means $t+\psi-n$, where n is the largest integer such that $t+\psi-n\geqslant 0$. Suppose that the firing occurs at a threshold phase θ_0 and that the next firing takes place after the time interval t_1. Then the next phase θ_1 can be written

$$\theta_1=\hat{\eta}(\theta_0)\equiv\eta(t_1;\theta_0) \tag{15}$$

If a phase-locking occurs for an initial condition, the sequence $\{\theta_n\}$ $(n>N)$ has a periodicity for a large natural number N.

Two examples of firing phase maps obtained numerically are shown in Fig. 3, and the dependency of phase-locking on the parameter k is illustrated in Fig. 4.

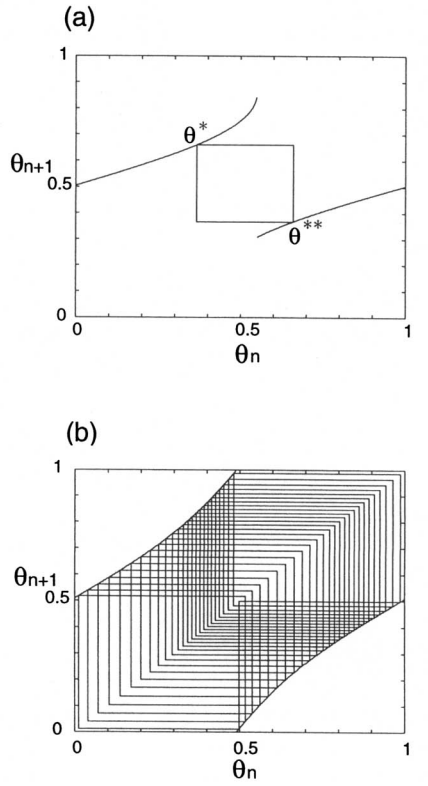

Fig. 3. Two examples of firing phase maps obtained numerically. Both graphs show $\{\theta_n\}$ $(n=101,\ldots,150)$ after 100 iterations of an initial phase. (a) a 1:2 phase-locking occurs, and after several iterations two phases θ^* and θ^{**} repeat in turn. $k=0.5$, $\tau=0.51$, and $\beta=2$. (b) quasi-periodic behavior. $k=0.1$, $\tau=0.51$, and $\beta=2$.

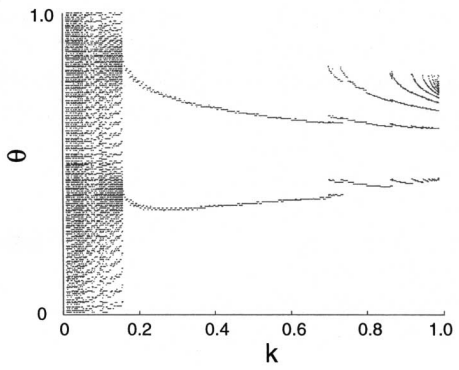

Fig. 4. Bifurcation diagram showing the dependency of phase-locking on the parameter k. The firing phase sequence $\{\theta_{1000},..., \theta_{1100}\}$ is illustrated. For a 1:2 phase-locking region, fixed phase relations are represented by two dots for each k value even though 101 points are actually concentrated on each of the two points. Since there is no such fixed phase relation for quasiperiodic cases (in the parameter range $0 < k < 1.7$), the dots are scattered throughout the phase domain spanning the interval [0 1). $\tau = 0.51$ and $\beta = 2$.

3. STOCHASTIC PHASE-LOCKINGS AND BIFURCATIONS

3.1. Stochastic Integrate-and-Fire Model

Now consider a system of a stochastic differential equations described by

$$dX(t) = \left\{ -\frac{1}{\tau} X(t) + \beta \right\} dt + \delta \, dW(t) \tag{16}$$

and

$$X(0) = 0 \tag{17}$$

instead of Eqs. (1) and (2). Here $W(t)$ denotes the standard Wiener process and represents an additive noise, which means that it is independent of the state variable $X(t)$, and the constant δ is a noise intensity. The time-dependent threshold is the same as that given by Eq. (4):

$$\phi(t) = 1 + k \sin\{2\pi(t + \theta_0)\} \tag{18}$$

The state point governed by Eqs. (16) and (17) is reset to zero as soon as the point reaches this time-varying threshold.

The problem of finding the time interval when the oscillator with an additive noise reaches the threshold is reduced to the first-passage-time problem of the Ornstein–Uhlenbeck process with a time-varying boundary. Making use of the probability density functions (pdf's) of the first-passage-time, we can define a stochastic firing phase map, referred to in this case as a stochastic kernel, and an operator that governs the transition of the threshold phase density after the oscillator reaches the threshold. Phase-lockings in a stochastic sense can then be investigated on the basis of the density evolution of the operator.

The rest of this subsection gives some definitions necessary for the following discussion. By $L^1(C)$ shall be denoted the class of functions f on the circle C such that

$$\|f\| = \int_C |f(x)|\, dx < \infty \tag{19}$$

Then $\|f\|$ is the $L^1(C)$ norm of f. As is customary, we will say that $h \in L^1(C)$ is a density if h is non-negative and its integral over the domain C is equal to unity. Let the set $\mathscr{D}$ of pdf's be defined by

$$\mathscr{D} = \{h \in L^1(C) \mid h \geqslant 0,\ \|h\| = 1\} \tag{20}$$

Denote by T_θ a time interval when the one-dimensional stochastic process $X(t)$ reaches the time-varying threshold $\phi(t)$ for the first time after leaving an initial point $X(0) = 0$ with an initial threshold phase $\theta \in C$. The time interval T_θ is a random variable representing a first-passage-time from the state point $X(0) = 0$ to the threshold $\phi(t)$.

Let $f_T(t; \theta)$ be the first-passage-time probability density function of a process $X(t)$ with an initial state $X(0) = 0$ and with an initial threshold phase $\theta \in C$:

$$f_T(t; \theta)\, dt = \text{Prob}\{t \leqslant T < t + dt \mid \Theta = \theta\} \tag{21}$$

From the above definition, we know that

$$\int_{t \in [0\ \infty)} f_T(t; \theta)\, dt = 1 \qquad \text{for} \qquad \theta \in C \tag{22}$$

Since Eq. (16) implies that $X(t)$ is the Ornstein–Uhlenbeck process,[2] the numerical procedure proposed by Buoncore *et al.*[11] can be used to compute the first-passage-time pdf in the case of a time-dependent boundary.

---

[2] Strictly speaking, the random varialble $X(t)$ of Eq. (16) is not the Ornstein Uhlenbeck process because it contains an additive drift term β.

3.2. Stochastic Kernels and Operators

To describe the motion of a state point in terms of the phase of the threshold, we can transform the pdf of the first-passage-time T into that of the threshold phase as follows: for $\theta_0 \in C$,

$$g(\theta \mid \theta_0) = \sum_{\eta(t_i;\, \theta_0) = \theta} \frac{f_T(t_i;\, \theta_0)}{|\eta'(t;\, \theta_0)|} = \sum_{\eta(t_i;\, \theta_0) = \theta} f_T(t_i;\, \theta_0) \tag{23}$$

where $\eta'(t;\, \theta)$ means $\partial\eta(t;\, \theta)/\partial t$. The pdf $g(\theta \mid \theta_0)$ of the variable θ describes the transformation probability of a given threshold phase θ_0. Hence, a map V: $\theta_0 \to \theta$ whose transformation pdf is subjected to $g(\theta \mid \theta_0)$ corresponds to a deterministic firing phase map $\hat{\eta}$ in a stochastic sense.

Now let the initial boundary phase θ_0 be distributed on C according to a probability density function $h_0(\theta_0) \in \mathscr{D}$. After a state point reaches the threshold, the pdf of the threshold phase $h_1(\theta)$ is described by

$$h_1(\theta) = \int_C g(\theta \mid \theta_0)\, h_0(\theta_0)\, d\theta_0 \tag{24}$$

or $h_1 = \mathscr{P} h_0$ and $h_1 \in \mathscr{D}$, where $\mathscr{P}$: $\mathscr{D} \to \mathscr{D}$ is an integral operator defined by

$$\mathscr{P} h_0(\theta) = \int_C g(\theta \mid \theta_0)\, h_0(\theta_0)\, d\theta_0 \tag{25}$$

For any given pdf h_0 we can make use of the operator $\mathscr{P}$ to define h_n ($n = 1, 2, \ldots$) inductively:

$$h_n = \mathscr{P} h_{n-1} = \mathscr{P}(\mathscr{P} h_{n-2}) = \cdots \mathscr{P}^n h_0 \tag{26}$$

If $\mathscr{P}$ is the operator defined above and if

$$\mathscr{P} h^* = h^* \tag{27}$$

for some $h^* \in \mathscr{D}$, then h^* is called an invariant density of the operator $\mathscr{P}$. We can now define the asymptotic stability of a sequence of density functions $\{\mathscr{P}^n h_0\}$ in the following way. For every $h_0 \in \mathscr{D}$, a sequence $\{\mathscr{P}^n h_0\}$ is said to be asymptotically stable if there exists a unique invariant density h^* and

$$\lim_{n \to \infty} \| \mathscr{P}^n h_0 - h^* \| = 0 \tag{28}$$

From the definition of $g(\theta \mid \theta_0)$, we know that the inequality for $a > 0$ and $a \in C$,

$$\int_C \inf_{0 \leqslant \theta_0 \leqslant a} g(\theta \mid \theta_0) > 0 \tag{29}$$

holds.[5] Therefore, the sequence $\{\mathscr{P}^n h_0\}$ is asymptotically stable (Corollary 5.7.1 in ref. 12).

Also from the definition of $g(\theta \mid \theta_0)$ we know that this function of the operator satisfies the conditions

$$\int_C g(\theta \mid \theta_0)\, d\theta = 1 \tag{30}$$

and

$$g(\theta \mid \theta_0) \geqslant 0 \tag{31}$$

That is, $g(\theta \mid \theta_0) \in \mathscr{D}$ (c.f., Eq. (20)). A function of an operator satisfying Eqs. (30) and (31) is, in general, called a stochastic kernel.[12] Even in the deterministic case the kernel $K(\theta, \theta_0)$ can be formally defined by using a delta function $\delta(\cdot)$ and a firing phase map $\hat{\eta}$ of Eq. (15):

$$K(\theta, \theta_0) = \delta[\theta - \hat{\eta}(\theta_0)] \tag{32}$$

In general, if a kernel $K(x, y)$ satisfies Eq. (30) and Eq. (31) for $x, y \in C$, the eigenvalues and eigenfunctions of $K(x, y)$ can be found. The eigenfunction problem for a $K(x, y)$ is to find eigenvalues λ and eigenfunctions $\xi(\cdot)$ satisfying

$$\int_C K(x, y)\, \xi(y)\, dy = \lambda \xi(x) \tag{33}$$

For any stochastic kernel K the following results are known.[13]

KI. $\lambda = 1$ is an eigenvalue for K, and all eigenvalues λ satisfy

$$|\lambda| \leqslant 1 \tag{34}$$

KII. If $\xi(\cdot)$ is an eigenfunction of K with the eigenvalue $|\lambda| = 1$, then $|\xi(\cdot)|$ is the eigenfunction with the eigenvalue 1.

KIII. If there is an eigenfunction of K with eigenvalue $|\lambda| = 1$ and there is no degeneracy for the eigenvalue 1, there is an integer N such that

$\lambda^N = 1$. This means that all eigenvalues of absolute value 1 are Nth roots of unity.

These properties are discussed in the following subsection, where a transition probability matrix replaces a stochastic kernel.

Even if we do not derive the analytical form of the kernel of $g(\theta \mid \theta_0)$, we can study the characteristics of the kernel numerically. The two examples of numerically calculated stochastic kernels illustrated in Fig. 5 correspond to the deterministic firing maps in Fig. 3. One is a 1:2 phase-locking kernel, and the other is a quasi-periodic kernel.

The following section provides some examples of pdf evolutions whose densities are asymptotically stable and discusses the stochastic phase-lockings in terms of pdf evolutions. Figure 6 shows two examples of pdf evolutions (h_1, h_2, h_3 and h^*) from a uniform initial distribution (h_0). The stochastic kernels in Fig. 5 were used in calculating these evolutions, and the pdf h^* represents function h_{10000} because the exact invariant density in these cases cannot be calculated.

3.3. Markov Chains

The previous section observed the transition of a state point indirectly, through the pdf's evolution, given an initial phase density of the firing threshold phase. This section takes a direct look at a movement of a state point θ_n on C at a time step n.

We can first define a state space, denoted by $\{S_i\}$ $(i = 1,..., N_s)$, which is a finite set of equal disjoint intervals on C:

$$S_i = \{\theta \mid (i-1)/N_s \leqslant \theta < i/N_s\} \qquad (i = 1,..., N_s) \tag{35}$$

For simplicity, state S_i shall be identified with state i. We can refer to the values of Y_n as the position of a state point at a time step n and it is customary to speak of Y_n being in state i if $Y_n = i$, which means that a state point θ_n is in state S_i at n.

Before analyzing of the transition probability matrix of a Markov chain, we should consider some general properties of a *stochastic matrix*. If all the elements in a real square matrix A are non-negative (or positive) and the sum of all the elements in each column is unity, that is, if

$$a_{ij} \geqslant 0 \qquad (i, j = 1, 2,..., N_a) \tag{36}$$

$$\sum_{j=1}^{N_a} a_{ij} = 1 \qquad (i = 1, 2,..., N_a) \tag{37}$$

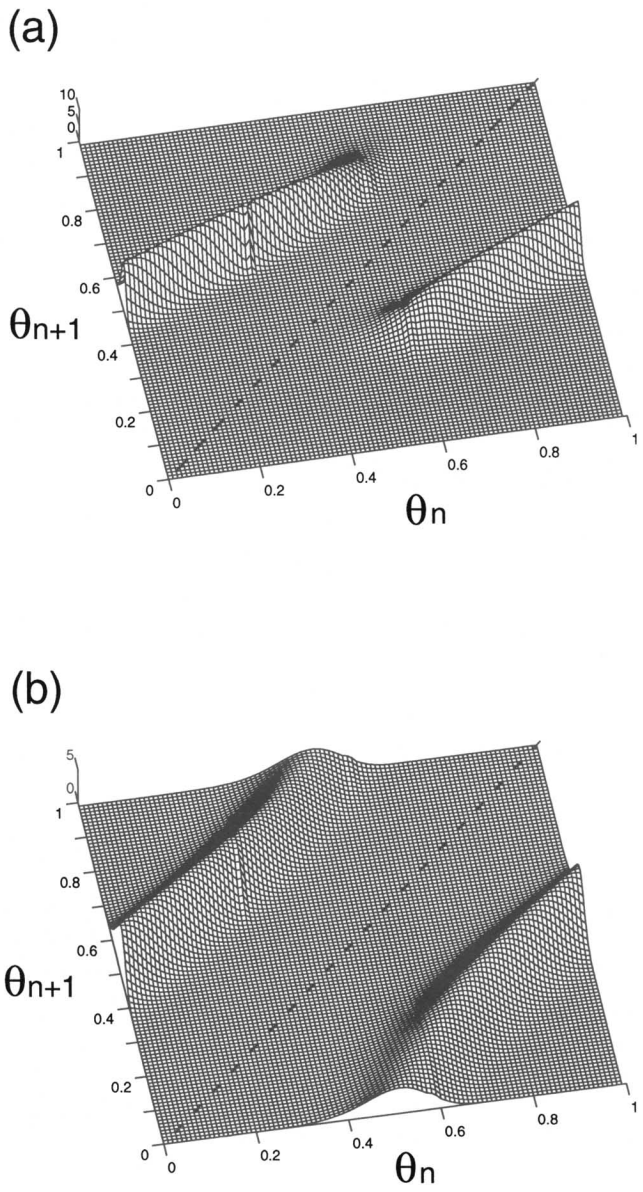

Fig. 5. Numerically calculated stochastic kernels $g(\theta_{n+1}|\theta_n)$ corresponding to the deterministic firing maps in Fig. 3. (a) a stochastic kernel corresponding to a 1:2 phase-locking in the deterministic case: $k=0.5$, $\tau=0.51$, $\beta=2$, and $\delta=0.2$. (b) a quasi-periodic stochastic kernel: $k=0.1$, $\tau=0.51$, $\beta=2$, and $\delta=0.2$.

then A is called a stochastic matrix.[14] As a matter of convenience, suppose that characteristic values $\{\lambda_i\}$ $(i=0, 1, ..., N_a-1)$ of A are sorted in descending order according to their moduli:

$$|\lambda_0| \geqslant |\lambda_1| \geqslant \cdots \geqslant |\lambda_{N_a-1}| \tag{38}$$

A stochastic matrix has the following specific properties:

AI. If a stochastic matrix is irreducible, it has a real and positive characteristic value 1 which is a simple root of the characteristic equation. No characteristic value has a modulus greater than 1.

AII. To the maximal characteristic value 1 there corresponds a characteristic vector with positive coordinates.

AIII. If A has k characteristic values $\lambda_0=1, \lambda_1, \lambda_2, ..., \lambda_{k-1}$ of modulus 1, then these numbers are all distinct and are roots of the equation

$$\lambda^k - 1 = 0 \tag{39}$$

More generally, the whole spectra $\lambda_0, \lambda_1, \lambda_2, ..., \lambda_{k-1}$ of A, regarded as a system of points in the complex λ-plane, goes over into itself under a rotation of the plane by the angle $2\pi/k$. The properties AI, AII, and AIII respectively correspond to KI, KII, and KIII.

In our case, the transition probabilities are completely determined by a stochastic kernel $g(\theta \mid \theta_0)$. That is,

$$\begin{aligned} p_{ij}^{\{n, n+1\}} &= \text{Prob}\{ Y_{n+1}=j \mid Y_n=i \} \\ &= \text{Prob}\{ \theta_{n+1} \in S_j \mid \theta_n \in S_i \} \\ &= \int_{\theta_n \in S_i} \int_{\theta_{n+1} \in S_j} g(\theta_{n+1} \mid \theta_n)\, d\theta_{n+1}\, d\theta_n, \qquad (i, j=1, ..., N_s) \end{aligned} \tag{40}$$

The transition probabilities $p_{ij}^{\{n, n+1\}}$ $(i, j=1, ..., N_s)$ are independent of the values n and $n+1$, $p_{ij}=p_{ij}^{\{n, n+1\}}$ $(i, j=1, ..., N_s)$, and $P=(p_{ij})$ is a stochastic matrix.

We know from Eq. (29) that all elements of the transition probability matrix P are positive:

$$p_{ij} > 0 \qquad (i, j=1, ..., N_s) \tag{41}$$

Therefore any two states i and j communicate: the process is thus irreducible (more precisely, the process is primitive because all elements of

P are possitive). All states then communicate with each other, and P has only one recurrent class. Since the transition probability is that of a finite Markov chain with period 1, the process is also aperiodic. It is also known that if a finite Markov chain is irreducible and aperiodic, it has a unique invariant (or stationary) probability distribution $\pi = (\pi_1, ..., \pi_{N_s})$.[15, 16]

As mentioned above, a stochastic matrix in general has the characteristic value 1, and so does the transition probability matrix P. The

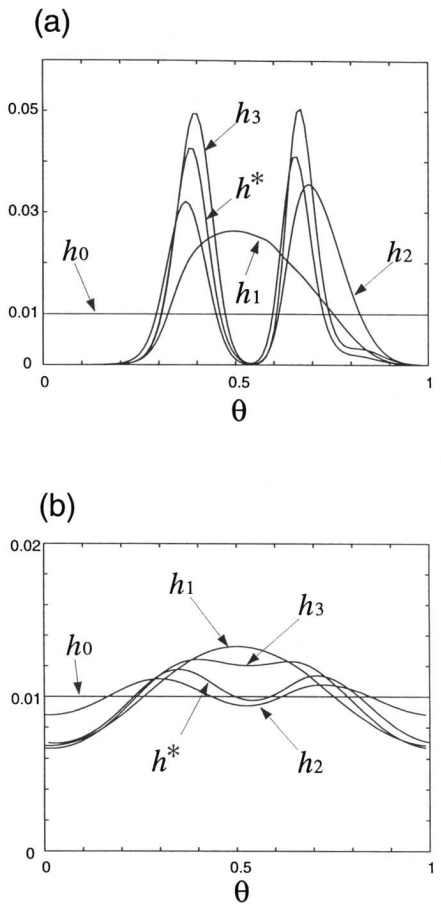

Fig. 6. Examples of pdf evolutions (h_1, h_2, h_3 and h^*) from a uniform initial distribution (h_0). Each stochastic kernel in Fig. 5 is used, and both evolutions are asymptotic stable cases. The pdf h^* represents a function h_{10000} because the exact invariant density in these cases cannot be calculated. (a) evolution corresponding to a 1:2 phase-locking in the deterministic case: $k = 0.5$, $\tau = 0.51$, $\beta = 2$, and $\delta = 0.2$. (b) evolution corresponding to a quasi-periodic behavior in the deterministic case: $k = 0.1$, $\tau = 0.51$, $\beta = 2$, and $\delta = 0.2$.

multiplicity of the characteristic value 1 is, in this case, unity because it is equal to the number of recurrent classes associated with the finite Markov matrix P. Furthermore, since the transition probability matrix P is a finite irreducible aperiodic Markov chain, according to Theorem 3.2 in Chapter 4 of ref. 16, there are no other characteristic values of modulus 1 except for unity ($\lambda_0 = 1$). This means that the matrix P does not have roots of the equation $\lambda^k - 1 = 0$ except for $\lambda = 1$.

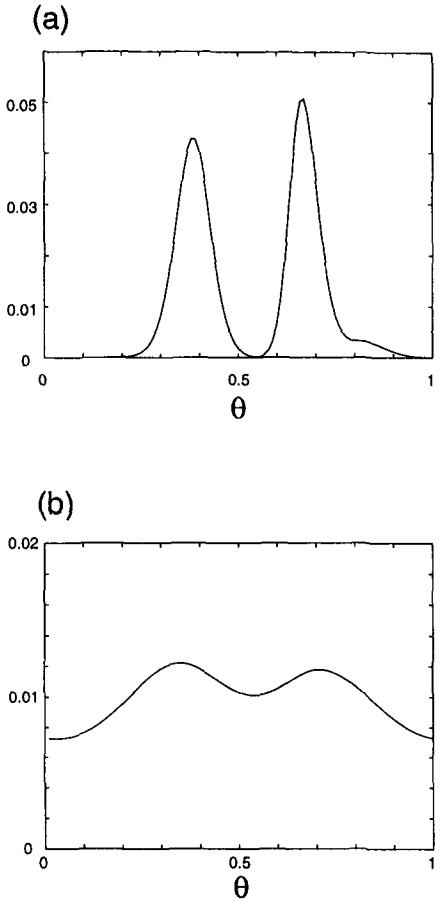

Fig. 7. Characteristic vectors (eigenfunctions) which belong to the characteristic value $\lambda_0 = 1$ of each kernel in Fig. 5. These functions are coincident with the invariant densities (h^*) illustrated in Fig. 6. (a) the stochastic kernel corresponding to a 1:2 phase-locking in the deterministic case. $k = 0.5$, $\tau = 0.51$, $\beta = 2$, and $\delta = 0.2$. (b) a stochastic quasi-periodic kernel: $k = 0.1$, $\tau = 0.51$, $\beta = 2$, and $\delta = 0.2$.

4. NUMERICAL ANALYSIS

4.1. Spectral Analysis of Stochastic Kernels

The integral operator $\mathscr{P}$ governs evolution properties of a sequence $\{h_n\}$, and a kernel g of the operator has all the information needed to describe the dynamical evolution. This section therefore analyzes the spectral properties of the kernel: eigenfunctions and eigenvalues. For a

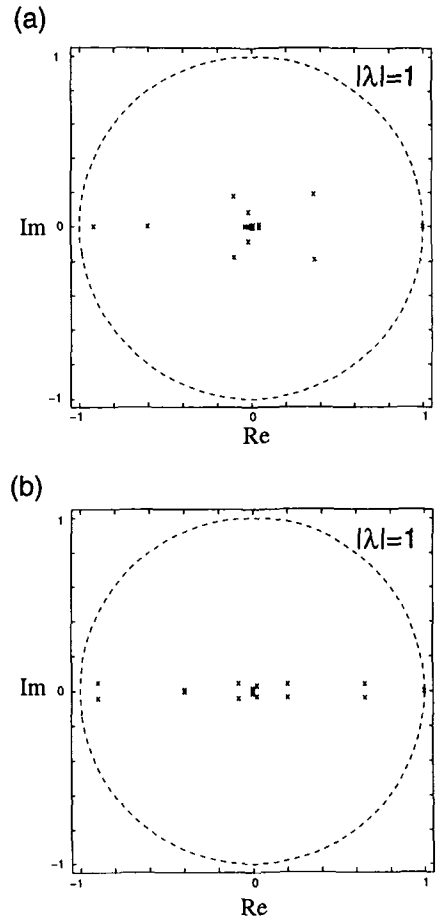

Fig. 8. Examples of the whole spectrum of characteristic values of the stochastic kernels are illustrated in the complex plane. Each of the kernels has a unique characteristic value $\lambda_0 = 1$. (a) a stochastic kernel corresponding to a 1:2 phase-locking in a deterministic case: $k = 0.5$, $\tau = 0.51$, $\beta = 2$, and $\delta = 0.2$. (b) a stochastic quasi-periodic case: $k = 0.1$, $\tau = 0.51$, $\beta = 2$, and $\delta = 0.2$.

stochastic kernel g we can obtain a numerical representation denoted by a square matrix $M=(m_{ij})$ $(i, j=1,..., N_m)$. We should note, however, that from a numerical point of view Eqs. (36) and (37) are not actually satisfied. Some m_{ij} $(i, j=1,..., N_m)$, for instance, may be zero and some $\sum_{j=1}^{n} m_{ij}$ $(i=1, 2,..., N_m)$ may not be exactly unity. Note that the speed of the convergence of the sequence $\{h_n\}$ to its invariant density is determined by the characteristic values other than the first characteristic value ($\lambda_0=1$). Therefore, since several of the following characteristic values play an important role, we should pay particular attention to the second and third characteristic values.

Figure 7 shows two characteristic vectors which belong to the first characteristic value of each kernel in Fig. 5, and these functions are coincident with the invariant densities illustrated in Fig. 6. Hence, the following part of this paper uses as the invariant density the characteristic vector (eigenfunction) of the first characteristic value of the matrix M.

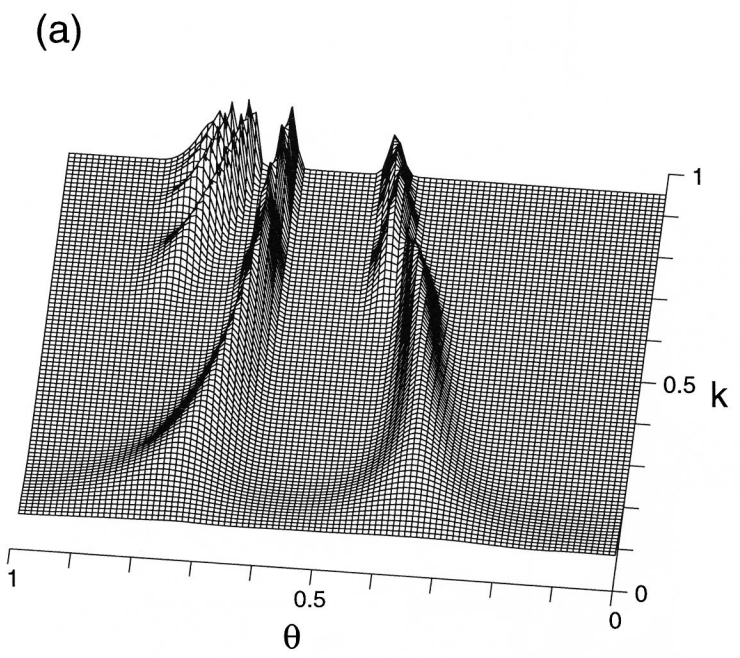

Fig. 9. (a) Invariant density diagram for a noise intensity $\delta=0.1$ and corresponding to the deterministic bifurcation diagram in Fig. 4: $\tau=0.51$ and $\beta=2$. Invariant densities h^* are plotted for each of 90 equally spaced k values on the interval [0.05 0.95]. (b) the second and third characteristic values' moduli versus k. (c) the second and third characteristic values' angles versus k.

In Fig. 8 two examples of the whole spectrum of characteristic values of the kernel of an operator $\mathscr{P}$ are shown in the complex plane for $N_m = 100$. Each of the operators has a unique characteristic value $\lambda_0 = 1$. Parts (a) and (b) respectively correspond to the deterministic 1:2 phase-locking and quasi-periodic cases, and each stochastic kernel is the same as that corresponding part of Fig. 5.

Figures 9 through 12 show, for various noise intensities ($\delta = 0.1$, 0.36, 0.37, and 1.0), the invariant density diagram (which corresponds to stochastic bifurcation diagram in ref. 5) as well as of the moduli and angles of the second and third characteristic values (λ_1 and λ_2) plotted against k.

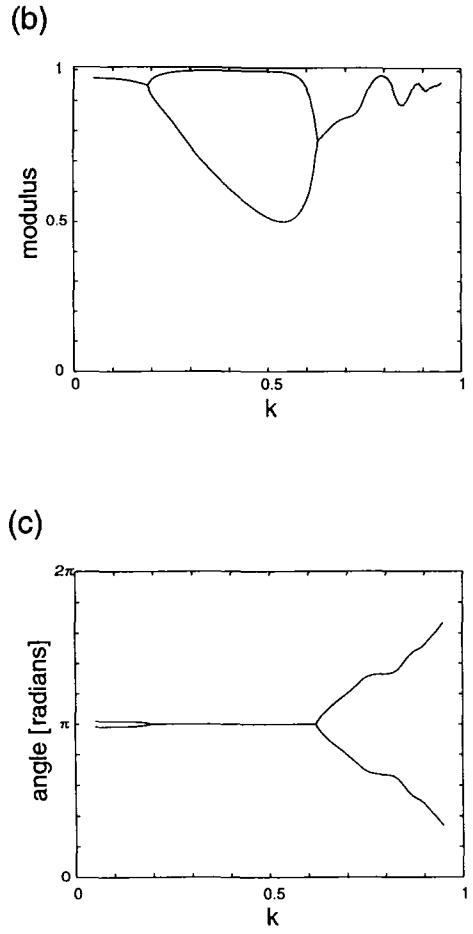

Fig. 9. (*Continued*)

The structure of the invariant density diagram with the noise intensity $\delta = 0.1$ (Fig. 9) looks like that of the diagram for the deterministic case (c.f., Fig. 4). We can see that near $k = 0.19$ the second and third characteristic values change from complex to real. This implies the bifurcation from the quasi-periodic behavior to 1:2 phase-locking occurs in a stochastic sense. We refer to the point at which this happens as the stochastic bifurcation point. Near $k = 0.63$, on the other hand, the Values change from real to complex. In the parameter range $0.19 < k < 0.63$, the angle of the characteristic values is exactly π radians. Note that each invariant density function has the same topological structure, with two peaks in this parameter range (c.f., Fig. 7(a)). As the parameter k increases beyond this range the angles of the second and third characteristic values depart from each other. We can see that around $k = 0.8$ two characteristic values are almost invariant under rotation through an angle of $2\pi/3$ in the complex plane. This constancy implies that this is a case of stochastic 1:3 phase-locking.

Comparing parts (b) and (c) of Figs. 9 and 10, we find that the point of bifurcation from stochastic quasi-periodic behavior to stochastic 1:2

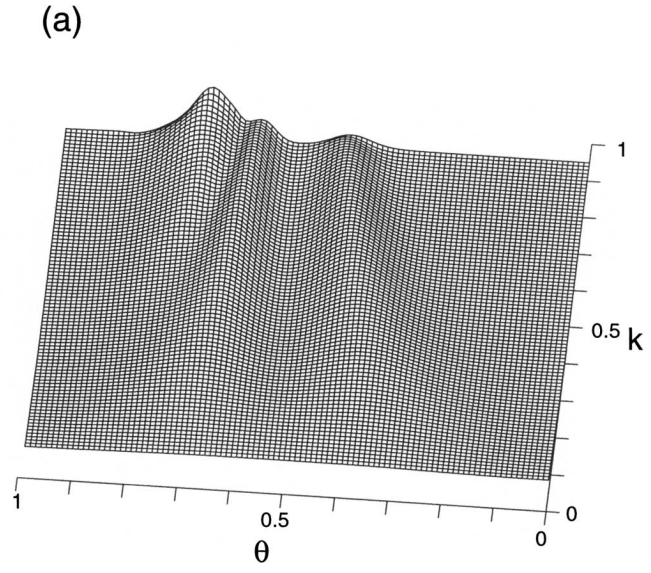

Fig. 10. (a) Invariant density diagram for a noise intensity $\delta = 0.36$ and corresponding to the deterministic bifurcation diagram in Fig. 4: $\tau = 0.51$ and $\beta = 2$. Invariant densities h^* are plotted for each of 90 equally spaced k values on the interval [0.05 0.95]. (b) the second and third characteristic values' moduli versus k. (c) the second and third characteristic values' angles versus k.

phase-locking shifts leftward as the noise intensity increases. In Fig. 11 there are no real second or third characteristic values (λ_1 and λ_2) in the entire range of the parameter k. Though the topological structures of the invariant density diagrams in Fig. 10(a) and Fig. 11(a) do not seem to be greatly different from each other, we can find the quantitative change by making use of the spectral analysis.

As the noise intensity increases, the structure of the invariant density diagram becomes flatter and there are no real second and third characteristic values when the noise intensity is high (Fig. 12).

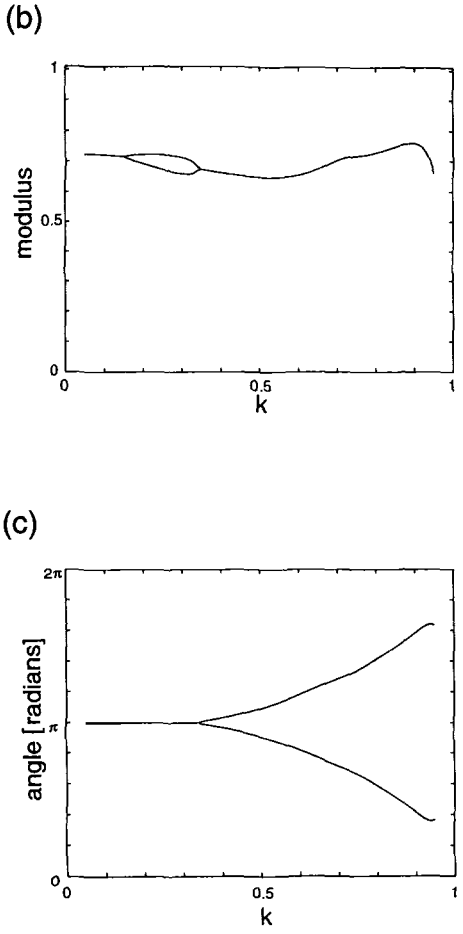

Fig. 10. (*Continued*)

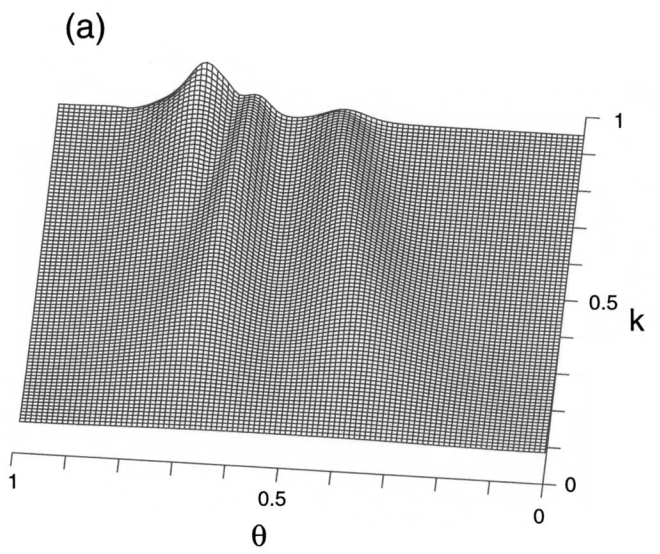

Fig. 11. (a) Invariant density diagram for a noise intensity $\delta = 0.37$ and corresponding to the deterministic bifurcation diagram in Fig. 4: $\tau = 0.51$ and $\beta = 2$. Invariant densities h^* are plotted for each of 90 equally spaced k values on the interval [0.05 0.95]. (b) the second and third characteristic values' moduli versus k. (c) the second and third characteristic values' angles versus k.

4.2. Transition Probability Matrix

The transition probability matrix of a Markov process, and hence the process itself, can be graphically represented by a transition diagram formed of nodes and directed line segments called branches. Each node is numbered to represent one state i ($i = 1,..., N_s$) of the process. A directed line segment (branch) is drawn from each node i to each node j. Furthermore, since we have seen that all the elements of the transition probability matrix P of Markov chains are positive, we shall consider a diagram showing only those directed line segments with transition probabilities p_{ij_k} ($i = 1,..., N_s$, $k = 1,..., w(i)$) for which the following equations hold for each i:

$$p_{ij_1} \geqslant p_{ij_2} \geqslant \cdots \geqslant p_{ij_{Ns}} \tag{42}$$

$$\sum_{k=1}^{w(i)-1} p_{ij_k} < 0.95 \tag{43}$$

$$\sum_{k=1}^{w(i)} p_{ij_k} \geqslant 0.95 \tag{44}$$

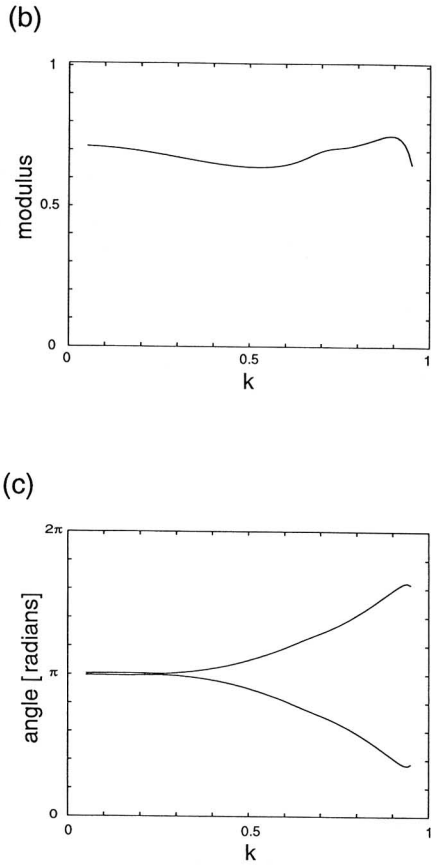

Fig. 11. (*Continued*)

This diagram will be called a *pseudo-transition diagram*. Because the row elements of the matrix with segments satisfying Eqs. (42), (43), and (44) sum to more than 0.95, the numbers on all the branches leaving a node must also sum to more than 0.95.

Consider pseudo-transition diagrams (not shown here) in which the unit circle C has been divided into 10 states (i.e., $N_s = 10$) and which correspond to the stochastic kernels in Fig. 5. If the parameters correspond to a deterministic 1:2 phase-locking case, the invariant density of the operator $\mathscr{P}$ has sharp peaks in states 4 and 7 (c.f., Fig. 6(a)), and all states move to the two states in high transition probabilities. On the other hand, if the parameters correspond to a deterministic quasi-periodic case, each state tends to transit to its diagonal states. Thus there are no sharp peaks

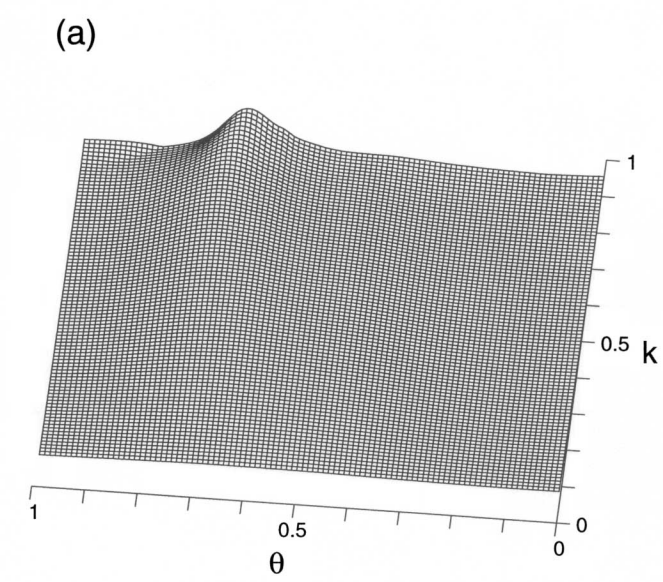

Fig. 12. (a) Invariant density diagram for a noise intensity $\delta = 1.0$ and corresponding to the deterministic bifurcation diagram in Fig. 4: $\tau = 0.51$ and $\beta = 2$. Invariant densities h^* are plotted for each of 90 equally spaced k values on the interval [0.05 0.95]. (b) the second and third characteristic values' moduli versus k. (c) the second and third characteristic values' angles versus k.

in the invariant density (c.f., Fig. 6(b)). In Fig. 13, for $N_s = 10$ two examples of the whole spectrum of characteristic values $(\lambda_0, ..., \lambda_9)$ of transition matrices are shown in the complex plane. In this figure each of the matrices has a unique characteristic value $\lambda_0 = 1$ and parts (a) and (b) respectively correspond to the stochastic 1:2 phase-locking and stochastic quasi-periodic kernels of Fig. 5. Comparing this figure with Fig. 8 (for stochastic kernels), we find that the configurations of the first several characteristic values in the corresponding parts of the two figures are quite similar.

5. DISCUSSION

The integrate-and-fire type oscillator with a periodic threshold is one of the simplest models of biological oscillators but is nonetheless very useful when we want to analyze the stochastic aspects of the dynamical structure of biological oscillations. This paper quantitatively evaluated stochastic bifurcations and phase-lockings by exploiting a spectral analysis of stochastic kernels. This method makes it clear that the locations of stochastic bifurcation points in the parameter space depend on the noise

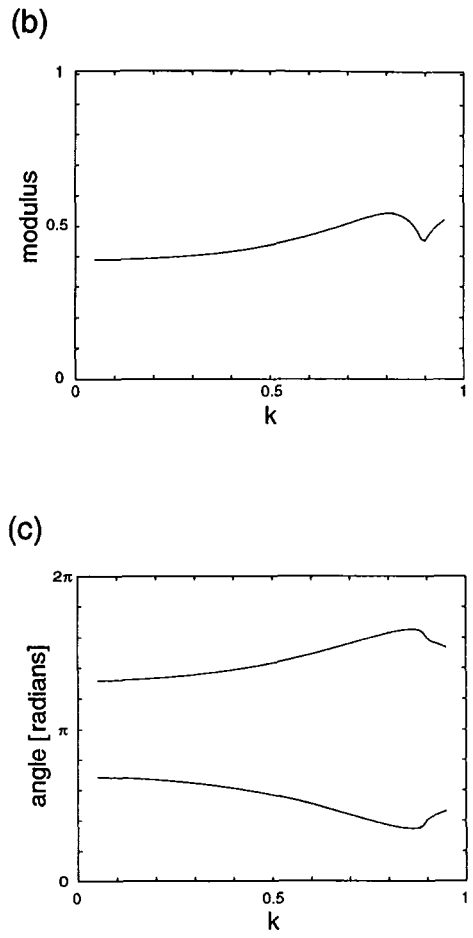

Fig. 12. (*Continued*)

intensity. Moreover, the method is easy to apply because the numerical calculation it uses does not require the solving of stochastic differential equations. "Noisy" nonlinear dynamical systems have recently received attention, and the method used in this paper should be extended to other nonlinear systems.

APPENDIX A. PHASE-LOCKING REGIONS

To determine the boundary of the M:1 phase-locking regions, we look for phase-locked solutions of Eq. (7). Because the critical cases can occur

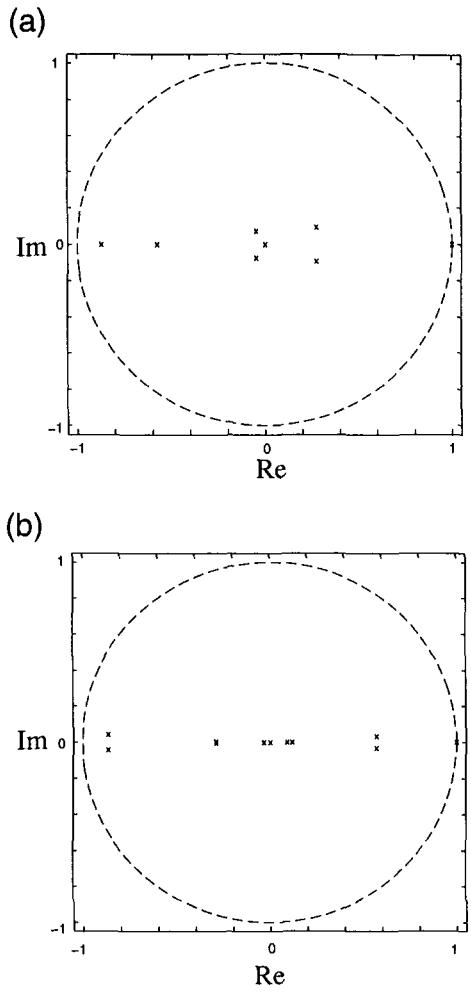

Fig. 13. Examples of the whole spectrum of characteristic values for the transition probability matrices are shown in the complex plane. Each of the matrices has a unique characteristic value $\lambda_0 = 1$. (a) a 1:2 phase-locking parameters in the deterministic case: $k = 0.5$, $\tau = 0.51$, $\beta = 2$, and $\delta = 0.2$. (b) a stochastic quasi-periodic case: $k = 0.1$, $\tau = 0.51$, $\beta = 2$, and $\delta = 0.2$.

on the boundary of these regions, we need to find solutions of Eq. (7) that satisfy $t_{n+1} = t_n + M$ and that disappear when arbitrarily small changes of parameter values are made.

If the function F is monotonic—that is, when $\tau\beta - 1 > k\sqrt{1 + (2\pi\tau)^2}$ (Region I)—and the function f of Eq. (12) is continuous. Roots of the equation

$$F(t_n + M) = G(t_n) \tag{45}$$

can disappear only in pairs when two roots coalesce. Thus a critical case occurs when

$$F'(t_n + M) = G'(t_n) \tag{46}$$

Since

$$F(t + M) = \exp(M/\tau)\, F(t) \tag{47}$$

$$G(t) = \tau G'(t) \tag{48}$$

by deleting the function $G(t)$ from the conditions specified by Eqs. (45) and (46), we can reduce them to

$$F(t_n) - \tau F'(t_n) = 0 \tag{49}$$

By straightforward elimination we find that

$$\sin(t_n + \gamma) = 1 \tag{50}$$

Substituting Eq. (50) for Eq. (45), we find

$$k = |\tau\beta(1 - \exp(-M/\tau)) - 1| \tag{51}$$

It is now convenient to introduce a constant τ_0 such as

$$\tau_0 = -\left[\log\left(1 - \frac{1}{\tau\beta}\right)\right]^{-1} \tag{52}$$

if $\tau\beta > 1$. This constant is equal to $\tau_0 = \tau/t^*$, where t^* satisfies

$$\tau\beta\{1 - \exp(-t^*/\tau)\} = 1 \tag{53}$$

The t^* is the time the state point reached a time-invariant threshold $\phi(t) = 1$ for the first time.

Using τ_0 we can rewrite Eq. (51) as

$$k = \left| \frac{1 - \exp(-M/\tau)}{1 - \exp(-1/\tau_0)} - 1 \right| \tag{54}$$

The second critical case occurs when the $F(t)$ is not monotonic—when $k\sqrt{1 + (2\pi\tau)^2} > |\tau\beta - 1|$ (Region II). Fixed points of the mapping Eq. (7) can then be lost because of the discontinuity. Thus a critical case occurs when Eq. (7) holds and $F'(t_n) = 0$. When a root moves to the right into the discontinuity, these two conditions give us the critical curves bounding the phase-locking region:

$$k = \left[\left\{ \frac{\exp(-M/\tau)}{2\pi\tau} \right\}^2 + \left\{ \frac{1 - \exp(-M/\tau)}{1 - \exp(-1/\tau_0)} - 1 \right\}^2 \right]^{1/2} \tag{55}$$

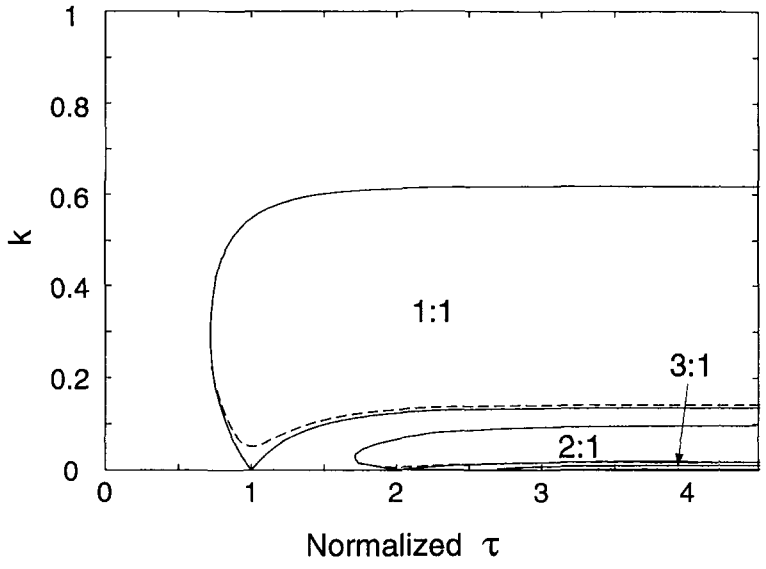

Fig. 14. Phase-locked regions in the $(\tau/\tau_0, k)$ space for a fixed parameter $\beta = 2$. The border of the M:1 phase-locking patterns (indicated by the solid line) was computed by using Eq. (51) in Appendix A. Within this M:1 phase-locked region the dashed line computed by using Eq. (55) separates the region in which there is one solution (above the dashed line) from the region in which there are two solutions (below the dashed line).

If a root of Eq. (7) disappears into the discontinuity from the right, there are smaller values (t^*, $t_{n+1} - 1 < t^* < t_{n+1}$) for which

$$F'(t^*) = 0 \tag{56}$$

$$F(t^*) = G(t_n) \tag{57}$$

These conditions cannot be solved analytically, so what is plotted in Fig. 14 is their numerical solution.

In the regions between the 1:1 and 2:1 regions there are variety of other patterns (3:2, 4:3, 5:3, and so on), and there are in fact an infinite number of stable phase-locking patterns in regions of the parameter space between any two phased-locked regions.[10] Numerical studies also indicate that the firing patterns in phase-locked regions are independent of the initial conditions.[9]

APPENDIX B. NUMERICAL EXAMPLES OF THE TRANSITION PROBABILITY MATRIX AND THE INVARIANT DENSITIES

The transition probabilities that describe a Markov process are represented by an N_s-by-N_s transition matrix P with elements p_{ij}. Examples of the matrices in Section 4 can be calculated numerically for $N_s = 10$. For $k = 0.5$, $\delta = 0.2$, $\tau = 0.51$, and $\beta = 2$, we have

$$P = \begin{bmatrix}
* & * & * & * & 0.185 & 0.806 & 0.009 & * & * & * \\
* & * & * & * & 0.007 & 0.877 & 0.115 & * & * & * \\
* & * & * & * & * & 0.432 & 0.562 & 0.004 & * & * \\
* & * & 0.001 & 0.001 & * & 0.029 & 0.874 & 0.092 & 0.002 & * \\
0.001 & * & 0.007 & 0.024 & 0.002 & * & 0.394 & 0.533 & 0.038 & 0.001 \\
* & 0.001 & 0.055 & 0.260 & 0.024 & * & 0.012 & 0.448 & 0.190 & 0.011 \\
* & 0.001 & 0.061 & 0.654 & 0.189 & * & * & 0.017 & 0.068 & 0.010 \\
* & * & 0.006 & 0.411 & 0.580 & 0.005 & * & * & * & * \\
* & * & * & 0.074 & 0.867 & 0.060 & * & * & * & * \\
* & * & * & 0.002 & 0.658 & 0.339 & * & * & * & *
\end{bmatrix}$$

where * represents a number less than 0.001. And for $k = 0.1$, $\delta = 0.2$, $\tau = 0.51$, and $\beta = 0.51$, we have

$$P = \begin{bmatrix} * & * & * & 0.003 & 0.214 & 0.602 & 0.170 & 0.011 & 0.001 & * \\ * & * & * & * & 0.010 & 0.346 & 0.523 & 0.110 & 0.010 & 0.001 \\ 0.002 & * & * & * & * & 0.031 & 0.435 & 0.421 & 0.095 & 0.014 \\ 0.032 & 0.007 & 0.001 & * & * & * & 0.057 & 0.414 & 0.366 & 0.123 \\ 0.186 & 0.068 & 0.014 & 0.001 & * & * & * & 0.060 & 0.322 & 0.348 \\ 0.347 & 0.282 & 0.109 & 0.015 & 0.001 & * & * & * & 0.036 & 0.211 \\ 0.121 & 0.349 & 0.381 & 0.126 & 0.010 & * & * & * & * & 0.013 \\ 0.004 & 0.080 & 0.389 & 0.432 & 0.093 & 0.004 & * & * & * & * \\ * & 0.001 & 0.078 & 0.479 & 0.394 & 0.048 & 0.001 & * & * & * \\ * & * & 0.001 & 0.118 & 0.579 & 0.021 & 0.021 & 0.001 & * & * \end{bmatrix}$$

In these cases the invariant densities π are respectively

$$\pi = (* \quad * \quad 0.024 \quad 0.282 \quad 0.172 \quad 0.023 \quad 0.328 \quad 0.134 \quad 0.034 \quad 0.004)$$

and

$$\pi = (0.075 \quad 0.087 \quad 0.107 \quad 0.118 \quad 0.111 \quad 0.105 \quad 0.113 \quad 0.111 \quad 0.094 \quad 0.078)$$

ACKNOWLEDGMENTS

I thank Dr. Nobuo Matsumoto and Dr. Akio Kawana (NTT Basic Research Laboratries) for giving me the chance to do this work. And it is a pleasure to acknowledge fruitful discussions with Professor Shunsuke Sato, Dr. Shinji Doi, Dr. Khashayar Pakdaman, Dr. Taishin Nomura (Osaka University), and Dr. Shin Suzuki (NTT Basic Research Laboratories).

REFERENCES

1. F. Moss and P. V. E. McClintock, *Noise in Nonlinear Dynamical Systems*, Vols. 1–3 (Cambridge University Press, Cambridge, 1987).
2. L. Arnold, Random dynamical systems, in *Dynamical Systems*, R. Johnson, ed. (Springer, 1994), pp. 1–43.
3. J. Grasman and J. B. T. M. Roerdink, Stochastic and chaotic relaxation oscillations, *J. Stat. Phys.* **54**:949–970 (1989).
4. T. Tateno, S. Doi, S. Sato, and L. M. Ricciardi, Stochastic phase lockings in a relaxation oscillator forced by a periodic input with additive noise: A first-passage-time approach, *J. Stat. Phys.* **78**:917–935 (1995).
5. S. Doi, J. Inoue, and S. Kumagai, Spectral analysis of stochastic phase lockings and stochastic bifurcations in the sinusoidally forced van der Pol oscillator with additive noise, *J. Stat. Phys.* **90**:1107–1127 (1998).
6. S. Kauffman, Measuring a mitotic oscillator: the arc discontinuity, *Bull. Math. Biol.* **36**:171–182 (1974).

7. J. P. Keener, On cardiac arrhythmias: AV conduction block, *J. Math. Biol.* **12**:215–225 (1981).
8. B. W. Knight, Dynamics of encoding in a population of neurons, *J. Gen. Bhysiol.* **59**:734–766 (1972).
9. L. Glass and M. C. Mackey, A simple model for phase locking of biological oscillators, *J. Math. Biology* 7:339–352 (1979).
10. J. P. Keener, F. C. Hoppensteadt, and J. Rinzel, Integrate-and-fire models of nerve membrane response to oscillatory input, *SIAM J. Appl. Math.* **41**:503–517 (1981).
11. A. Buoncore, A. G Nobile, and L. M. Ricciardi, A new integral equation for the evaluation of first-passage-time probability densities, *Adv. Appl. Prob.* **19**:784–800 (1987).
12. A. Lasota and M. C. Mackey, *Chaos, Fractals, and Noise: Stochastic Aspects of Dynamics*, 2nd ed. (Springer-Verlag, 1994), pp. 112–122.
13. S. Chang and J. Wright, Transitions and distribution functions for chaotic systems, *Phys. Rev. A* **23**:1419–1433 (1981).
14. F. R. Gantmacher, *The Theory of Matrices*, Vol. II (Chelsea Publishing Company, 1959), pp. 82–112.
15. W. Feller, *An Introduction to Probability Theory and Its Application*, Vol. I (John Wiley & Sons, 1968), pp. 372–423.
16. S. Karlin, *A First Course in Stochastic Processes* (Academic Press Inc., 1966), pp. 27–103.